

Proton and Alpha Particle Impact Single and Double Ionization of Fe

Geetanjali¹, Sandeep Kumar Prasad² & L K Jha³

¹Department of Physics, S R A P College, Barachakiya

²Department of Physics, M P Science College, Muzaffarpur.

³University Department of Physics,
B R Ambedkar Bihar University, Muzaffarpur.

E- mail- lalan_jha@yahoo.com

Abstract: *Theoretical calculations of proton and alpha particle impact single and double ionization of Fe have been performed in the Modified Binary Encounter Approximation. Direct double ionization cross sections have been calculated in the modified binary encounter model. Accurate expression of $\sigma_{\Delta E}$ (cross section for energy transfer ΔE) and Hartree-Fock velocity distributions for the target electrons have been used throughout the calculations. The present results of single ionization cross sections are in good agreement with the experimental observations in the case of throughout the energy range. The calculated cross sections differs from the experimental results in the low energy regions because the present approximation not exhibits better result in the low energy regions while in case of double ionization the calculated results are in excellent agreement with the experimental observations.*

PACS No. 34.80Dp.

Keywords: BEA, Hartree-Fock Approximation, Double ionization

1. Introduction

Ionization of atoms and molecules is one of the basic processes in atomic physics. Thus, it has been extensively studied both experimentally and theoretically. Due to the broad range of applications and also due to its role in the study of atomic collision dynamics, there have been great scope, both experimental and theoretical, to improve our understanding of the ionization processes resulting from ion-impact with atoms. The description of multiple ionization is far from the simple task mainly due to complexity of the many possible paths leading to it. For example double ionization of atoms by fast ions is usually understood in terms of three mechanisms [1].

In case of different multiple ionization processes, the double ionization is the most important as the main contributions to the total ionization of the target is given by single and double ionization processes. Theoretical calculations of double ionization cross sections are considered to be most significant because contribution from different physical processes e.g. – Inner Shell Ionization followed by Auger emission, resonance excitation, Double auto-ionization process etc. can be separately estimated at various impact energies. Keeping in view, the importance of the degree of ionization and convenience in calculations, we have considered it worthwhile to estimate theoretically separate contributions from the relevant physical processes leading to double ionization.

Theoretical calculations of direct double ionization cross section become extremely difficult as it is related to the four-body Coulomb potential in the final channel [2]. Some interesting theoretical calculations on single and multiple ionization of Noble gases atom by fast proton impact have been reported where contributions of electron capture to multiple ionization are negligible. Spranger and Kirchner [3] investigated the ionization processes for Ne and Ar using independent particle model. They have also considered time delayed Auger like electron emission processes on the basis of a straight forward

Statistical Model and have concluded that high projectile velocities multiple ionization is dominated by Auger like processes. Archubi et al. [4] have developed a many electron model for multiple ionization of heavy atoms by bare ion. It is based on the solution of transport equation for an ion travelling through an inhomogeneous electron density. Among different experimental investigations on metals, McCartney and his group members [5] has used a cross beam technique incorporating time of flight analysis and coincidence counting of the collision products to carry out an interesting work on processes involving electron capture and multiple ionization in collisions of fast H^+ and He^{2+} ions with ground states lead atoms. Measurements of this type are very complex and difficult, and probably for this reason the experimental data have been obtained in the limited energy ranges. They have also carried out calculations in an independent electron model for the processes experimentally investigated but unfortunately the arguments of the theoretical result with the experimental data is not satisfactory [6].

In the past, Binary Encounter Approximation (BEA) has been used successfully to calculate charged particle impact single and double ionization cross sections for atoms and ions. Gryzinski [7] reasonably considered two processes in the Double Binary Encounter Model to describe double ionization. In the first process, the two electrons may be ejected from the system by two successive encounters of the incident particles with the target electrons. Alternatively, the incident electron may knock out only one target electron and the second electron is removed by the first ejected electron. Kara et al. [6] also supported the idea of above mentioned two-step interaction to describe the process of direct double ionization. In spite of certain unrealistic features and unjustified simplification in Gryzinski's mathematical formulation for the process of double ionization, the idea of Double Binary Encounter process has proper physical justification (see Roy and Rai [8], Vriens [9]). Later on, Roy and Rai modified Gryzinski's theory of electron impact double ionization suitably. The results of double ionization cross sections, based on the modified model including contribution of indirect processes, was found to be in close agreement with the experimental data [10,11]. In these calculations, Hartree – Fock and hydrogenic velocity distribution were used while considering ejection of the first and the second target electron respectively. Recently, Jha and Roy [12, 13] and Minakshi et al. [14] used Hartree – Fock velocity distribution while considering the ejection of both electrons of the target in the calculation of direct double ionization cross section. H^+ and He^+ impact single and double ionization of Mg and Pb calculated in the BEA shows good agreement with the experimental data. Singh et al. [15] has calculated single and double ionization of Mg by H^+ and He^{2+} impact. They have compared their calculated cross sections with the experimental observation made by Shah et al. [16]. The calculations have been carried out in the energy region of 90 – 2000 keV / amu in which the experimental data are available. In these calculations, they have found that in case of calculating single ionization cross section, the contribution of 3d shell only.

In the case of heavy charged particle impact, Kumar and Roy [17,18] pointed out errors and obsequies in Gryzinski's theory for calculation of the process mentioned above and modified the mathematical frame work suitably. Keeping the fact mentioned above in mind, we consider it worthwhile to carry out calculations of H^+ and He^+ impact single and double ionization cross section for Fe (iron) atom in BEA using Hartree – Fock velocity distribution for the ejected electrons. This will enable us to analyze single and direct double ionization cross sections and to examine the contribution to direct double ionization from indirect physical process.

2. Methods of Calculation for Single Ionization

In the present work, we have used the accurate expression of $\sigma_{\Delta E}$ (cross section for energy transfer ΔE) as given by Vriens [19] for heavy charged particles incident on atoms. Following Catlow and McDowell [20], we have introduced two dimensionless variables s and t defined by $s^2 = \frac{v_1^2}{v_0^2}$ and $t^2 = \frac{v_2^2}{v_0^2}$ where v_1 and v_2 are the velocities in atomic units of the incident particle and the target electron respectively and $U = v_0^2$ where v_0 is the average of r.m.s. velocity of orbital electrons and U is the ionization potential of the target in Rydbergs. All other energies involved are also expressed in Rydbergs. In terms of these variables, the expressions of ionization cross section due to a projectile of unit charge for particular incident energy and particular velocity of bound electron are given by Kumar and Roy [17].

$$Q_i(s, t) = \frac{4}{s^2 U^2} \left[1 + \frac{2t^2}{3} - \frac{1}{4(s^2 - t^2)} \right], \quad 1 \leq 4s(s - t) \quad (1)$$

$$= \frac{2}{s^2 U^2 t} \left[\frac{1}{4(s + t)} + t + \frac{2}{3} \{ 2s^2 + t^2 - (1 + t^2)^{3/2} \} \right], \quad 4s(s - t) \leq 1 \leq 4s(s + t)$$

$$= 0, \quad 1 > 4s(s + t)$$

Numerical integration of the expression for $Q_i(s, t)$ has been carried out over Hartree Fock velocity distribution of the bound electron to obtain the ionization cross section. Thus the expression for heavy charged particle impact single ionization cross section for a particular shell of the target is given by

$$Q_i(s) = n_e Z^2 \int_0^\infty Q_i(s, t) f(t) U^{\frac{1}{2}} dt (\pi a_0^2) \quad (2)$$

where n_e is the number of equivalent electrons in the shell under consideration and $f(t)$ is the momentum distribution function for the bound electron which is defined as

$$f(t) = 4\pi t^2 U \rho_{nl}(U^{1/2}t) \quad (3)$$

here

$$\rho_{nl} = \frac{1}{2l+1} \sum_{m=-l}^{+l} [\psi_{nlm}(\chi)]^2 \quad (4)$$

where

$$\psi_{nlm}(\chi) = \frac{1}{(2\pi)^{1/2}} \int \phi_{nlm}(r) e^{ik \cdot r} dr \quad (5)$$

is the Fourier transform of the one electron orbital.

Complete wave function or Slater orbitals is given by

$$\phi_{nlm}(r) = N_{nl} R_{nl}(r) Y_{lm}(\Omega) \quad (6)$$

Where $R_{nl}(r)$ and N_{nl} are the analytical Hartree-Fock radial function and normalization constant given as

$$N_{nl} = [(2n)!]^{-\frac{1}{2}} (2\xi)^{n+1/2} \quad (7)$$

and

$$R_{nl} = r^{n-1} e^{-\xi r} \quad (8)$$

Spherical harmonic $Y_{lm}(\Omega)$ have different form depending upon the value of quantum numbers l, m . Inner shell electrons in heavy atoms have high velocity and they are relativistic in nature. Hence, relativistic effect plays an important role for such targets. In present work, ionization from valence shells and a few inner shells have only been considered. In these cases relativistic effects are expected to make insignificant contribution to ionization cross section. Keeping this fact in account we have used non relativistic wave function in the present work.

In the present calculations, momentum distribution functions for the bound electrons have been constructed using Hartree – Fock radial functions reported by Clementi and Roetti [21]. For shell radii and binding energies of electrons, quantum mechanical value of radial distance of maximum probability given by Desclaux[22] and quantum mechanical values of orbital energies given by Clementi and Roetti [21] have respectively been used in the calculation. Complete wave function of Slater Orbitals wave function is given by

$$\phi_{nlm}(r) = N_{nl} R_{nl}(r) Y_{lm}(\Omega) \quad (9)$$

3. Methods of Calculation for Double Ionization

Heavy charged particle impact total double ionization cross section $Q^{ii}(T)$ including the contribution from Auger emission Q_A^{ii} can be written as

$$Q^{ii}(T) = Q_D^{ii} + Q_A^{ii} \quad (10)$$

when Auger effect is ignored, the direct double ionization Q_D^{ii} can be given as

$$Q_D^{ii} = Q_{sc}^{ii} + Q_{ej}^{ii} \quad (11)$$

In accordance of the idea given by Gryzinski[7] in double Binary Encounter model, these cross sections involving integrals over energy transfer are given by

$$Q_{sc}^{ii} = \frac{n_e(n_e-1)}{4\pi\bar{r}^2} \int_{U_i+U_{ii}}^{\Delta E^{max}} \sigma_{\Delta E}(E_q) \left[\int_{U_{ii}}^{\Delta E^{max}} \sigma_{\Delta E}(E_q - \Delta E) d(\Delta E') \right] d(\Delta E) \quad (12)$$

and

$$Q_{ej}^{ii} = \frac{n_e(n_e-1)}{4\pi\bar{r}^2} \int_{u_i+u_{ii}}^{\Delta E^{max}} \sigma_{\Delta E} \left[\int_{u_{ii}}^{\Delta E-u_i} \sigma_{\Delta E}(\Delta E') d(\Delta E') \right] d(\Delta E) \quad (13)$$

The various symbols used in the above expressions have been defined by Gryzinski [15]. Here ΔE and $\Delta E'$ stand for energy transfer during the first and the second collisions respectively and \bar{r} denotes the mean distance between the electrons in the shell given by $\bar{r} = R/n_e^{1/3}$ (R being the radius of the shell of the target atom), u_i and u_{ii} are the first and second ionization potentials corresponding to ejection of the electrons from the target. The symbol E_q represents the energy of the projectile.

In terms of dimensionless variables s and t discussed earlier, the expression for $\sigma_{\Delta E}$ in the case of a projectile of unit charge is given by Kumar and Roy [17]

$$\sigma_{\Delta E} d(\Delta E) = \begin{cases} Ad(\Delta E); & \Delta E \leq 4su(s-t) \\ Bd(\Delta E); & 4su(s-t) \leq \Delta E \leq 4su(s+t) \\ 0; & \Delta E > 4su(s+t) \end{cases} \quad (14)$$

where

$$A = \frac{1}{s^2 u} \left(\frac{1}{(\Delta E)^2} + \frac{4t^2 u}{3(\Delta E)^3} \right)$$

and

$$B = \frac{2}{3t(\Delta E)^3} \left(8s - \frac{[(\Delta E + t^2 u)^{1/2} - tu^{1/2}]^3}{s^2 u^{3/2}} \right)$$

The expressions of the scattered and ejected part of the direct double ionization cross sections showing the relevant integrals involving energy transfer and Hartree – Fock velocity distributions for the ejection of the two electrons are given below.

$$Q_{sc}^{ii} = \frac{n_e(n_e - 1)Z^2}{4\pi\bar{r}^2} \left(\int_{t=0}^{s-\frac{1}{4s}} \left\{ \int_{u_i}^{4su_i(s-t)} A\alpha d(\Delta E) + \int_{4su_i(s-t)}^{4su_i(s+t)} B\alpha d(\Delta E) \right\} f(t)u_i^{\frac{1}{2}} dt \right. \\ \left. + \int_{t=s-\frac{1}{4s}}^{\infty} \int_{u_i}^{4su_i(s+t)} B\alpha f(t)u_i^{\frac{1}{2}} d(\Delta E) dt \right) (\pi a_0^2) \quad (15)$$

when $(s - \frac{1}{4s})$ is positive

and

$$Q_{sc}^{ii} = \frac{n_e(n_e - 1)Z^2}{4\pi\bar{r}^2} \times \left(\int_{t=\frac{1}{4s}-s}^{\infty} \int_{u_i}^{4su_i(s+t)} B\alpha f(t)u_i^{\frac{1}{2}} d(\Delta E) dt \right) (\pi a_0^2) \quad (16)$$

when $(s - \frac{1}{4s})$ is negative

In the above expressions

$$\alpha = \int_0^{\infty} Q_i(s, t) f(t) u_{ii}^{1/2} dt (\pi a_0^2) \quad (17)$$

and s' is given by

$$s'^2 = \begin{cases} \frac{E_q - \Delta E}{1836u_{ii}} \\ \frac{E_q - \Delta E}{7344u_{ii}} \end{cases} \text{upper one is for H}^+ \text{ impact and lower one is for He}^{2+} \text{ impact} \quad (18)$$

Similarly equations for ejected part are

$$Q_{ej}^{ii} = \frac{n_e(n_e - 1)Z^2}{4\pi\bar{r}^2} \left(\int_{t=0}^{s-(1+\frac{u_{ii}}{u_i})/4s} \left\{ \int_{u_i+u_{ii}}^{4su_i(s-t)} A\alpha' d(\Delta E) + \int_{4su_i(s-t)}^{4su_i(s+t)} B\alpha' d(\Delta E) \right\} f(t)u_i^{\frac{1}{2}} dt \right. \\ \left. + \int_{t=s-\frac{(1+\frac{u_{ii}}{u_i})}{4s}}^{\infty} \int_{u_i+u_{ii}}^{4su_i(s+t)} B\alpha' f(t)u_i^{\frac{1}{2}} d(\Delta E) dt \right) (\Pi a_0^2) \quad (19)$$

whens $-\left(1 + \frac{u_{ii}}{u_i}\right)/4s$ is positive
and

$$Q_{ej}^{ii} = \frac{n_e(n_e - 1)Z^2}{4\pi\bar{r}^2} \times \left(\int_{t=\frac{(1+\frac{u_{ii}}{u_i})}{4s}-s}^{\infty} \int_{u_i+u_{ii}}^{4su_i(s+t)} B\alpha' f(t)u_i^{\frac{1}{2}} d(\Delta E) dt \right) (\pi a_0^2) \quad (20)$$

when $s - \left(1 + \frac{u_{ii}}{u_i}\right)/4s$ is negative with

$$\alpha' = \int_0^{\infty} Q_i(s', t) f'(t) u_{ii}^{1/2} dt (\pi a_0^2). \quad (21)$$

Here $Q_i(s', t)$ is the expression for electron impact ionization cross section of atoms Jha and Roy [12] and s' is given by $s'^2 = (\Delta E - u_i)/u_{ii}$ for both H^+ and He^{2+} impact.

Now we discuss the Z^2 dependence of the expression of Q_{sc}^{ii} which denotes a process in which the projectile knocks out two electrons successfully. In quantum mechanical approach this corresponds to a second order process, for which cross section scales as Z^4 . In this connection it is pertinent to point out the observations made by Vriens [17] that the two double binary encounter processes are linked with the quantum mechanical first and second order approximation. If one uses correlated many electron wave functions, direct double ionization cross section will be finite even in the first Born approximation. This has been assumed to correspond to Q_{ej}^{ii} of the process of direct double ionization. There is also a contribution to direct double ionization from the second Born approximation, which includes double processes like those represented by Q_{sc}^{ii} . In the present method the contributions of Q_{ej}^{ii} are found to be much smaller than those of Q_{sc}^{ii} Kumar and Roy [25,26]. In the case of proton impact $Z = 1$ and therefore, Z^4 scaling for Q_{sc}^{ii} becomes essentially the same as Z^2 scaling and good agreement of calculated results with the experiment is achieved. However, in the case of alpha particle impact, calculation involves $Z = 2$ and a Z^4 scaling of Q_{sc}^{ii} lead to much dominant contribution of this process adversely affecting the results. Hence the correspondence of the processes represented by Q_{ej}^{ii} and Q_{sc}^{ii} to the first and the second Born approximations does not appear to be suitable. In this context the experimental results of H^+ and He^{2+} impact pure double ionization cross sections are noteworthy. Beyond 100 keV/amu incident energy the graphical representations of cross sections for Fe and Cu show approximate Z^2 dependence of H^+ and He^{2+} impact pure double ionization cross sections Patton et al. [31]. From the experimental data of H^+ and He^{2+} ions incident on Fe and Cu targets, it is seen that the pure double ionization cross sections are about an order smaller than the corresponding single ionization cross sections which indicates usual trend of direct double ionization. Keeping these observations in view, we have assumed Z^2 dependence of direct double ionization cross sections in the present calculations as no established dependence of direct double ionization cross sections on Z is available for this purpose.

The integral appearing in Q_{sc}^{ii} and Q_{ej}^{ii} have been evaluated numerically. The functions $f(t)$ and $f'(t)$ appearing in the above equations are momentum distributions corresponding to the first and the second ejected electron respectively. These have been constructed from HF radial wave functions Catlow and McDowell [28], Jha and Roy [21]. We have considered total cross section for heavy charged particle impact direct double ionization of Fe (when sub-shells 4s, 3d and 3p are only considered) is given by

$$Q_D^{ii} = Q_D^{ii}(4s, 3d) + Q_D^{ii}(4s, 3p)$$

where $Q_D^{ii}(4s, 3d)$ and $Q_D^{ii}(4s, 3p)$ stand for the direct double ionization cross sections corresponding to ejection of one electron from 4s shell and the other either from the 3d shell or 3p shell respectively. The factor $n_e(n_e - 1)/4\pi\bar{r}^2$ has been suitably modified for considering the mode of ionization in which the electrons are ejected from different shells. Here $n_e(n_e - 1)$ has been replaced by $n_{e1} \times n_{e2}$ where these two stand for number of electrons in the shells under consideration. The binding energy of the shells of Fe, the expectation values of the shell radii and HF radial wave functions have been taken from the data reported by Clementi and Roetti [29].

4. Results and Discussion

(a) H^+ impact single ionization of Fe :

In the present theoretical investigation we have carried out the calculation of H^+ impact single ionization of Fe in the energy range 70 keV/amu to 1440 keV/amu. The results of calculated cross section along with experimental results of the single ionization have been shown in the Table 1 and Figure 1. In the case of H^+ impact single ionization of Fe we have taken only the contributions of 4s and 3d shells only. As shown in table the contribution of 3p is very small, hence its contribution has been ignored. Our calculated results are compared with the experimental investigation of Patton et al. [31]. The experimental observation clearly indicate that the lowest energy 70 keV/amu at which single ionization cross section has been measured is higher than the energy corresponding to the experimental maximum cross section. The experimental cross sections are found to decrease gradually with the increase of energy in the energy range 70 keV/amu to 1440 keV/amu. The calculated results show similar decreasing trend of cross sections with the increase in energy. At energy 70 keV/amu, the ratio of the theoretical to experimental cross section is 1.2. With the increase of the energy from 70 keV/amu to 500 keV/amu the ratio increases but it is always within a factor of 2 and at energies 600 keV/amu and 720 keV/amu the ratios are 2.02 and 2 respectively. It is quite surprising that at impact energy 420 keV/amu, a structure is found in the calculated result but such type of phenomenon has not been observed in the experimental result. At this energy the magnitudes of calculated cross sections and experimental measurements are $4.21 \times 10^{-16} \text{ cm}^2$ and $2.0 \times 10^{-16} \text{ cm}^2$ respectively, and their ratios are 2.10. Just the previous impact energy 355 keV/amu, the ratio of theoretical calculation to the experimental data is 2.03. This might be the reason behind the structure appeared in the graph at impact energy 420 keV/amu. Beyond this energy range the ratio of theoretical to the experimental results gradually falls and it is within a factor of 2 at impact energy 850 keV/amu. From the close inspection of the calculated results, it is found that 4s sub-shell contribution dominates at lower energy region while the 3d contribution is dominant at the higher energy region. The lowest energy considered in this calculation shows the value $9.06 \times 10^{-16} \text{ cm}^2$ while at this energy the experimental measured data shows the value $7.5 \times 10^{-16} \text{ cm}^2$. Thus our calculated value at lowest energy is in close agreement with the experimental findings both in magnitude and position. This tendency reflects that present results and the experimental cross sections are in close agreement both qualitatively and quantitatively throughout the energy range investigated.

(b) He^{2+} impact single ionization of Fe :

The calculated results of the He^{2+} impact single ionization of Fe along with the experimental data have been shown in the Table 2 and Figure 2. In the case of the alpha particle impact single ionization of Fe, we have considered the contributions of 4s, 3d, and 3p shells only. Since the contributions of 3s and other lower shells having magnitudes very small we have not taken the consideration of these shells. In this calculation we have calculated the cross sections from energy range 140 keV/amu to 1440 keV/amu and compared the results with experimental data of Patton et al. [31]. The contribution of 4s shell is highest at lowest energy while contribution of 3d shell is smallest at highest energies. In the experimental results, slight fluctuations have been seen at the energy 160 keV/amu having the magnitude $23.10 \times 10^{-16} \text{ cm}^2$. Except that from lower to higher energies the experimental cross section gradually decreases with the increase of energy and at highest energy 1440 keV/amu it becomes $6.70 \times 10^{-16} \text{ cm}^2$.

Similar trends have been seen in the calculated results also. At the lowest energy 140 keV/amu the magnitude of the calculated cross section is $14.63 \times 10^{-16} \text{ cm}^2$ while at highest energy 1440 keV/amu it becomes $6.99 \times 10^{-16} \text{ cm}^2$.

TABLE 1 : Proton impact single ionization cross section of Fe in unit of 10^{-16} cm^2

Energy (MeV)	Contributions of 4s shell	Contributions of 3d shell	Contributions of 3p shell	Contributions of (4s+3d) shells	Total	Expt. [23]
70	6.51	2.55	0.29	9.06	9.35	7.50
80	5.90	2.66	0.32	8.56	8.88	7.20
93	5.28	2.77	0.35	8.05	8.40	6.80
108	4.70	2.84	0.38	7.54	7.92	6.00
125	4.18	2.90	0.41	7.08	7.49	5.50
150	3.57	2.94	0.43	6.51	6.94	4.60
175	3.12	2.93	0.45	6.05	6.50	3.98
210	2.63	2.89	0.46	5.52	5.98	3.34
250	2.22	2.80	0.45	5.02	5.47	2.87
300	1.87	2.67	0.43	4.54	4.97	2.59
355	1.58	2.48	0.40	4.06	4.46	2.19
420	1.49	2.36	0.36	3.85	4.21	2.00
500	1.13	2.13	0.32	3.26	3.58	1.69
600	0.95	1.95	0.28	2.90	3.18	1.42
720	0.79	1.74	0.24	2.53	2.77	1.27
850	0.67	1.55	0.21	2.22	2.43	1.17
1000	0.57	1.30	0.19	1.87	2.06	0.98
1200	0.47	1.17	0.16	1.64	1.80	0.85
1440	0.40	1.00	0.14	1.40	1.54	0.71

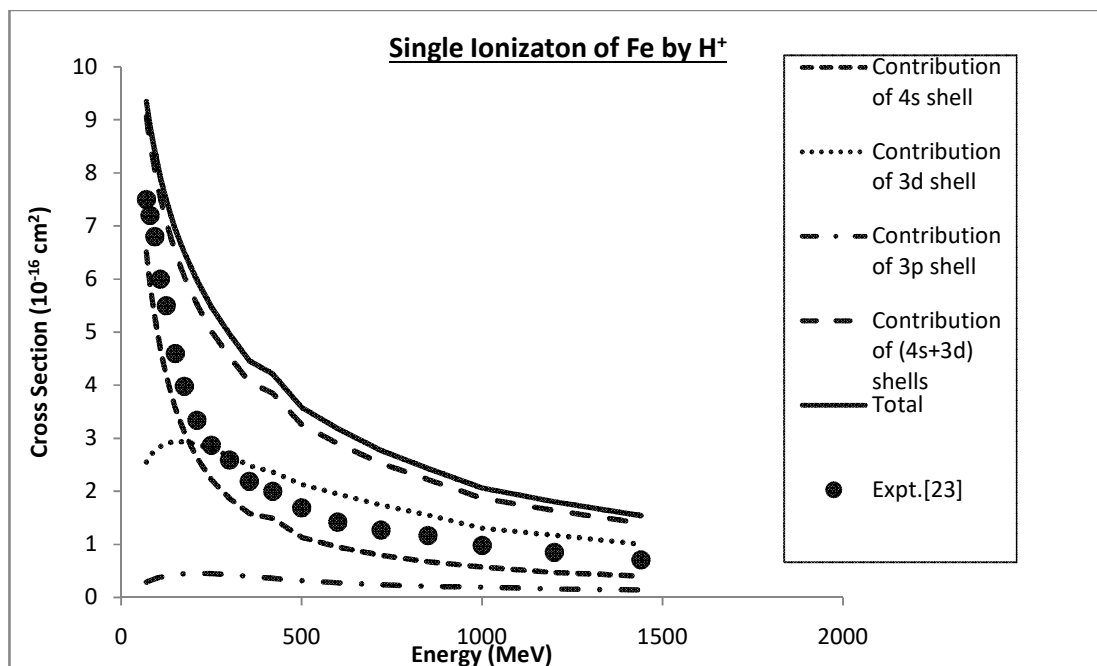
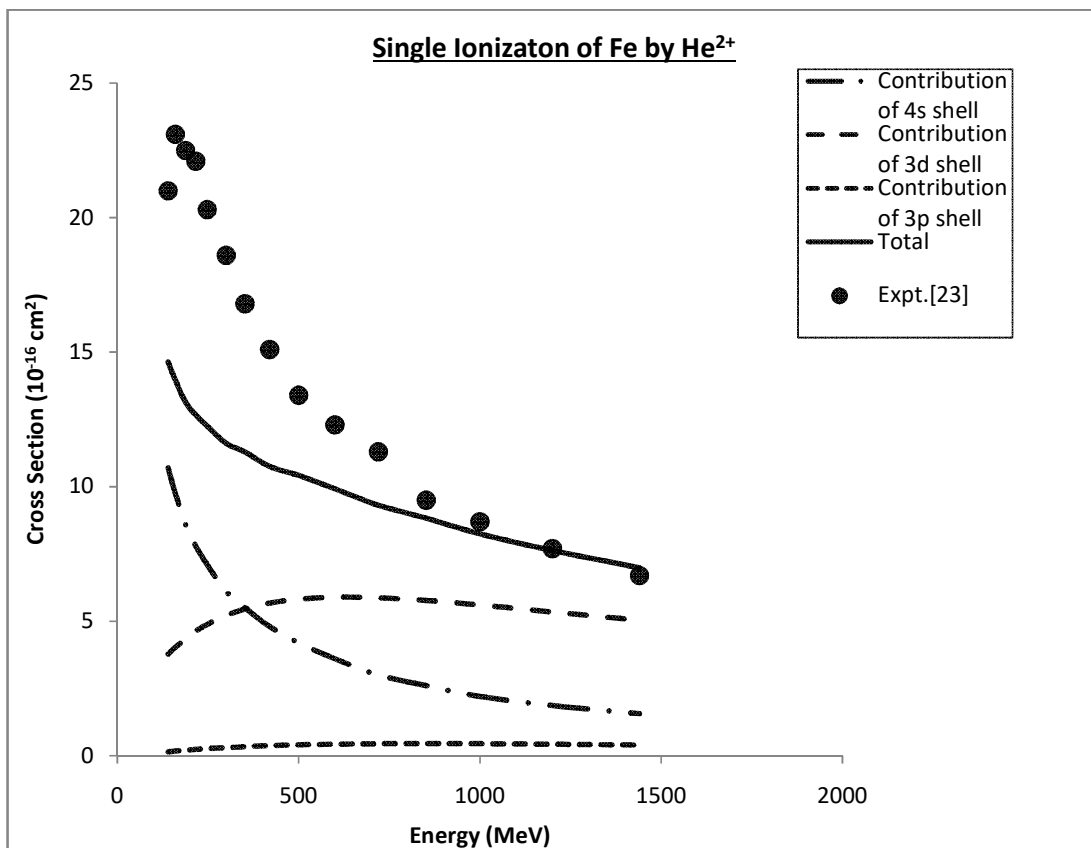
FIGURE 1: Proton impact single ionization cross section of Fe in unit of 10^{-16} cm^2 

TABLE 2 :Alpha impact single ionization cross section of Fe in the unit of 10^{-16} cm^2

Energy(MeV)	Contributions of 4s shell	Contributions of 3d shell	Contributions of 3p shell	Total	Expt.[23]
140	10.7	3.78	0.15	14.63	21.0
160	9.75	4.03	0.18	13.96	23.1
188	8.60	4.33	0.21	13.14	22.5
216	7.80	4.63	0.24	12.67	22.1
248	7.10	4.88	0.27	12.25	20.3
300	6.10	5.21	0.30	11.61	18.6
352	5.50	5.45	0.34	11.29	16.8
420	4.80	5.67	0.38	10.75	15.1
500	4.20	5.81	0.41	10.42	13.4
600	3.60	5.89	0.43	9.92	12.3
720	3.00	5.86	0.45	9.31	11.3
852	2.60	5.77	0.46	8.83	9.5
1000	2.20	5.60	0.45	8.25	8.7
1200	1.86	5.34	0.43	7.63	7.7
1440	1.56	5.03	0.40	6.99	6.7

FIGURE 2:Alpha impact single ionization cross section of Fe in the unit of 10^{-16} cm^2 

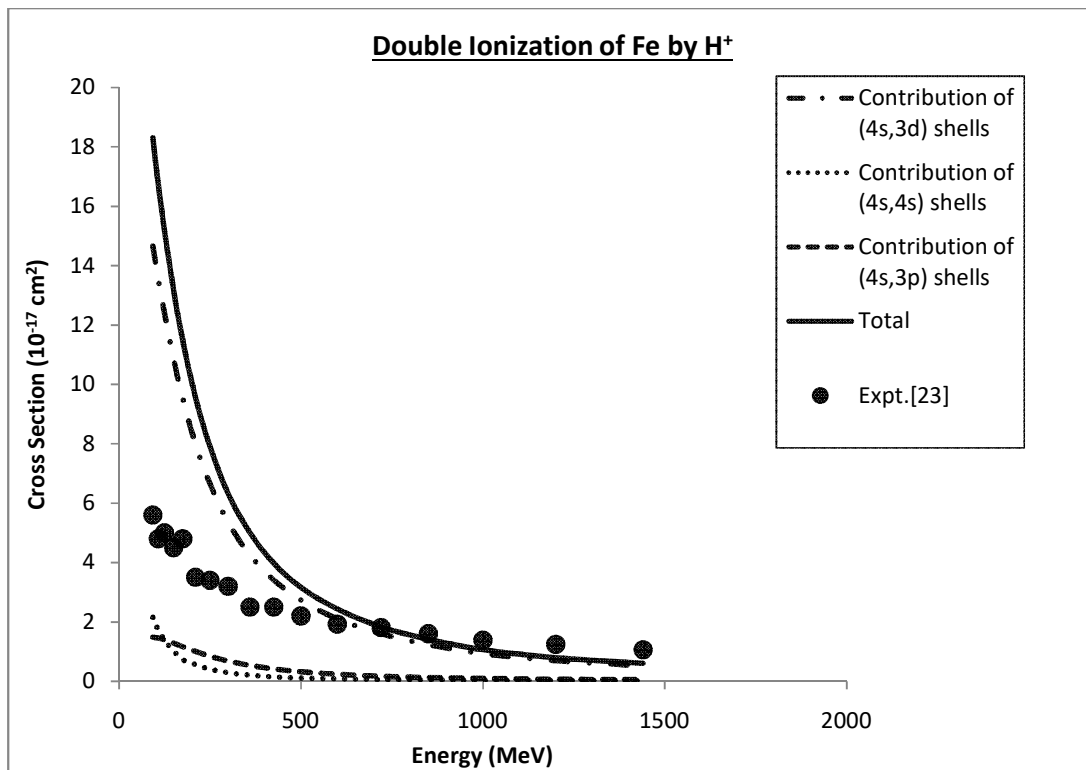
The experimentally measured cross section over-estimates throughout the calculated cross section except at energy 1440 keV/amu. At this energy the magnitude of the calculated cross sections and the experimental data are $6.99 \times 10^{-16} \text{ cm}^2$ and $6.70 \times 10^{-16} \text{ cm}^2$ respectively. It is surprising that in the case of alpha particle impact, the theoretical as well as experimental cross sections decreases slowly which is contrary to the results of proton impact single and double ionization of Fe. From the entire energy range which we have taken into account for the calculation it is found that with the increase of the energy both the cross sections gradually comes closer to each other and it becomes almost similar at the energy 1440 keV/amu. At this energy the ratio of the calculated cross section to the experimental data is 1.04. Magnitude of the experimental cross sections at lowest energy is almost three times greater compared to that of highest energy but in the case of calculated results the magnitude of cross sections at lowest energy is $14.63 \times 10^{-16} \text{ cm}^2$ while at highest energy considered the magnitude is $6.99 \times 10^{-16} \text{ cm}^2$ and it is more than two times larger than that of maximum energy taken into account. If we make comparison between such a trend of experimental as well as calculated cross sections it is found that the experimental cross sections decreases very rapidly with the increase of energy as compared to the calculated cross sections. When we closely inspect the calculated data to the experimental cross section, we find that there exist major random fluctuations. The discrepancies observed at low energy might be possible due to some other physical phenomenon. The calculated theoretical results major contributions have been observed due to 3d shell. The contribution of 3p shell is very small compared to 4s and 3d shells. The variation of the calculated results of 4s shell is much higher and it is almost more than 6 times between lowest and highest cross section taken into account. But, in the case of 3d shell contribution the lowest to highest cross section is more than 1.5 times. Contributions of these two shells (4s, 3d) indicate that the calculated cross sections decreases slowly in case of 3d shell while it is much faster in the case of 4s shell. Other major differences observed in the calculation of 4s and 3d shells is that in case of 4s shell the calculated results falls very fastly with the increase of the energy while in the case of 3d shell the situation is different in compared to 4s shell. A flat peak is observed in the calculation of both 3d and 3p shells. At impact energy 600 keV/amu, the magnitude is $5.89 \times 10^{-16} \text{ cm}^2$ in case of 3d shell while in case of 3p shell the peak is slightly shifted towards low energy regions and it is observed at impact energy 852 keV/amu having magnitude $0.46 \times 10^{-16} \text{ cm}^2$. We know that the 4s electrons are lost first during ionization. The electrons lost first will come from the highest energy level, furthest from the influence of the nucleus. So the 4s orbital must have a higher energy than the 3d orbital. The 3d orbital is technically lower in energy and closer to the nucleus than 4s orbital because it is at energy level 3. That is the reason behind the calculated cross sections falls much faster in case of 4s shell while it is gradually decreases in case of 3d and 3p shells respectively.

(c) H^+ impact Double ionization of Fe :

In the case of H^+ impact double ionization of Fe we have taken the contributions of (4s, 4s), (4s, 3d) and (4s, 3p) shells. We have compared our calculated results with the experimental data of Patton et al. [31] from the energy range 93 keV/amu to 1440 keV/amu which have been shown in the Table 3 and Figure 3. In our calculated results we found that the contributions of (4s, 4s), (4s, 3d) and (4s, 3p) having magnitudes $2.16 \times 10^{-17} \text{ cm}^2$, $14.66 \times 10^{-17} \text{ cm}^2$ and $1.49 \times 10^{-17} \text{ cm}^2$ at impact energy 93 keV/amu. At this energy the magnitudes of experimental and theoretical results are $5.60 \times 10^{-17} \text{ cm}^2$ and $18.31 \times 10^{-17} \text{ cm}^2$ respectively. The ratio of the theoretical calculation to the experimental data is 3.26 at the lowest energy. Both the experimental data and the calculated cross sections are highest at the lowest energy while it gradually decreases with the increase of energies considered. At low energy the theoretical results dominates to the experimental data while with the increase of energy the calculated results decreases rapidly as compared to the experimental measurements. With the increase of energy both the results are coming closer to each other and at the energy 720 keV/amu it is almost similar. At this energy the calculated result is of magnitude $1.84 \times 10^{-17} \text{ cm}^2$ and the experimental data is of the magnitude $1.81 \times 10^{-17} \text{ cm}^2$. Beyond this energy the magnitude of the calculated results gradually decreases as compared to the magnitude of experimental data. At the highest energy 1440 keV/amu magnitude of calculated result is $0.61 \times 10^{-17} \text{ cm}^2$ while the experimental data is of magnitude $1.06 \times 10^{-17} \text{ cm}^2$. At this energy the ratio of calculated results to the experimental data is 0.57. From the energy range 93 keV/amu to 250 keV /amu the results are beyond the factor of 2. But with the increase of energy both the results are coming closer to each other.

TABLE 3 : Proton impact double ionization cross sections of Fe in unit of 10^{-17} cm^2

Energy (MeV)	Contributions of (4s,3d) shells	Contributions of (4s,4s) shells	Contributions of (4s,3p) shells	Total	Expt.[23]
93	14.66	2.16	1.49	18.31	5.60
108	13.55	1.74	1.46	16.75	4.80
125	12.42	1.39	1.40	15.21	5.00
150	10.88	1.03	1.29	13.20	4.50
175	9.55	0.73	1.17	11.51	4.80
210	8.01	0.57	1.01	9.59	3.50
250	6.66	0.41	0.85	7.92	3.40
300	5.36	0.29	0.68	6.33	3.20
360	4.26	0.21	0.54	5.01	2.50
425	3.42	0.15	0.42	3.99	2.50
500	2.74	0.11	0.32	3.17	2.20
600	2.11	0.09	0.24	2.44	1.92
720	1.61	0.06	0.17	1.84	1.81
850	1.24	0.05	0.13	1.42	1.60
1000	0.94	0.03	0.10	1.07	1.38
1200	0.70	0.03	0.07	0.80	1.24
1440	0.53	0.02	0.06	0.61	1.06

FIGURE 3: Proton impact double ionization cross sections of Fe in unit of 10^{-17} cm^2 

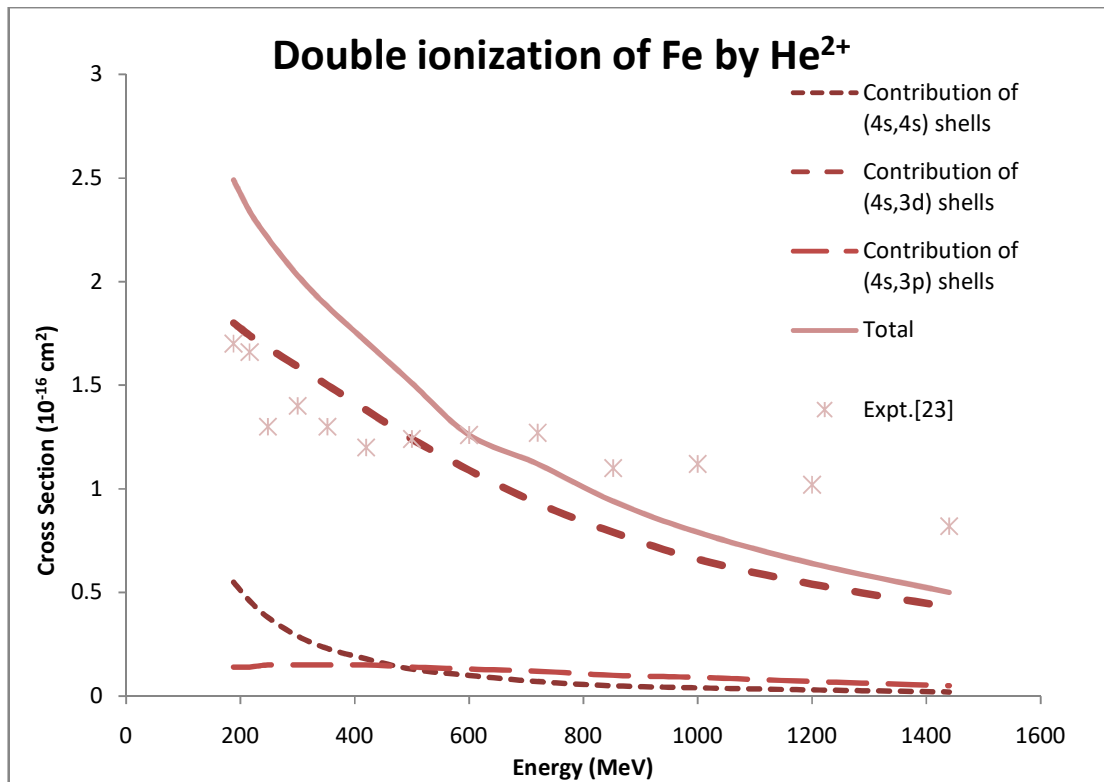
From the energy range 360 keV/amu to 1440 keV/amu the results are within the factor of two. From the close inspection the magnitude of experimental measurement decreases slowly while the magnitudes of theoretical results are decreasing very rapidly. The ratio of calculated cross section to the experimental data is more than three times at given lowest impact energy (say 93 keV/amu) while it is near about 0.57 at highest impact energy (say 1440 keV/amu) respectively. The over-estimation of the calculated results at low energy range is the usual feature of our calculation (i.e. following BEA). The ratio of the calculated cross section to the experimental measurements are 2.0, 1.44, 1.01, 0.88, 0.64 and 0.57 at impact energies 360 keV/amu, 500 keV/amu, 720 keV/amu, 850 keV/amu, 1200 keV/amu, and 1440 KeV/amu respectively. At these energies from 360 keV/amu to 1440 keV/amu the magnitudes of the calculated results are $5.01 \times 10^{-17} \text{ cm}^2$, $3.17 \times 10^{-17} \text{ cm}^2$, $1.84 \times 10^{-17} \text{ cm}^2$, $1.4 \times 10^{-17} \text{ cm}^2$, $0.80 \times 10^{-17} \text{ cm}^2$ and $0.61 \times 10^{-17} \text{ cm}^2$ and that of experimental results are $2.5 \times 10^{-17} \text{ cm}^2$, $2.2 \times 10^{-17} \text{ cm}^2$, $1.81 \times 10^{-17} \text{ cm}^2$, $1.6 \times 10^{-17} \text{ cm}^2$, $1.24 \times 10^{-17} \text{ cm}^2$ and $1.06 \times 10^{-17} \text{ cm}^2$ respectively. From the discussion given above it clearly indicates that with the increase of energy the results are coming closer to each other and are within the factor of two and supposed to be in good agreement with the experimental results.

(d) He^{2+} impact Double Ionization of Fe :

In the calculation of He^{2+} impact double ionization of Fe, we have calculated the cross sections from the energy range 188 keV/amu to 1440 keV/amu and compared with the experimental data of Patton et al. [31] which have been shown in the Table 4 and Figure 4. In this calculation we have taken the contributions of (4s, 4s), (4s, 3d) and (4s, 3p) shells only. In this calculation from the lower energy range from 188 keV/amu to 500 keV/amu, the calculated cross sections over-estimate the experimental data. Beyond this energy the calculated cross sections under-estimates the contributions of the experimental cross sections up to the highest energy which we have considered except at 600 keV/amu. The over-estimation of the calculated cross sections at low energy range is the usual trend of BEA. The ratio of the calculated cross sections to the experimental measured data is almost within the factor of two and it becomes identical at energy of 600 keV/amu. At the lower energies 188 keV/amu, 216 keV/amu, 300 keV/amu the ratios of calculated to experimental cross sections are 1.46, 1.40 and 1.45 respectively. But at the energies 600 keV/amu, 852 keV/amu, 1200 keV/amu and 1440 keV/amu the ratio of the calculated cross sections to the experimental data are 1.0, 0.85, 0.62 and 0.60 respectively. The experimental cross sections at lowest energy 188 keV/amu has a magnitude $1.7 \times 10^{-16} \text{ cm}^2$ while at the highest energy 1440 keV/amu it becomes $0.82 \times 10^{-16} \text{ cm}^2$.

TABLE 4 :Alpha particle impact double ionization cross section of Fe in unit of 10^{-16} cm^2

Energy(MeV)	Contributions of (4s,4s) shells	Contributions of (4s,3d) shells	Contributions of (4s,3p) shells	Total	Expt.[23]
188	0.55	1.80	0.14	2.49	1.70
216	0.46	1.74	0.14	2.34	1.66
248	0.38	1.68	0.15	2.21	1.30
300	0.29	1.59	0.15	2.03	1.40
352	0.23	1.50	0.15	1.88	1.30
420	0.18	1.38	0.15	1.71	1.20
500	0.13	1.24	0.14	1.51	1.24
600	0.10	1.09	0.13	1.26	1.26
720	0.07	0.93	0.12	1.12	1.27
852	0.05	0.79	0.10	0.94	1.10
1000	0.04	0.66	0.09	0.79	1.12
1200	0.03	0.54	0.07	0.64	1.02
1440	0.02	0.43	0.05	0.50	0.82

FIGURE 4: Alpha impact double ionization cross sections of Fe in unit of 10^{-16} cm^2 

The ratio of the experimental data of lowest cross section to the highest cross section is almost doubled while the ratio of the lowest calculated cross section to the highest cross section is almost five times greater which indicates that the fall in magnitude of the experimental cross sections decrease slowly while the calculated cross sections fall rapidly with the increase of energy as compared to the experimental findings.

References

1. McGuire, J. H.; *Double Ionization of He by protons and electrons at high velocities*, *Phys. Rev. Lett.*, **1982**, 49, 1153
2. Berakdar, J.; *Positron and Electron impact double ionization of He at low and intermediate energies*, *Phys. Lett. A*, **1996**, 220,237
3. Spranger, T.; Kirchner, T.; *Auger like processes in multiple ionization of Noble gas atoms by protons*, *J. Phys. B : At. Mol. Opt. Phys.*, **2004**, 37, 4159
4. Archubi, C. D.; Montanari, C. C.; Mirangola, J. E.; *Many electron model for multiple ionization in atomic collisions*, *J. Phys. B : At. Mol. Opt. Phys.*, **2007**,40, 943
5. McCartney, P. C. E.; Shah, M. B.; Geddes J.; Gilbody, H. B.; *Processes involving electron capture and multiple ionization in collisions of fast H^+ and He^{2+} ions with lead atoms*, *Phys. Rev. A*, **1999**, 60,4582
6. Kara, V.; Paludam, K.; Moxom, J.; Ashley, P.; Laricchia, G.; *Single and Double ionization of Ne, Kr and Xe by positron impact*, *J. Phys. B : At. Mol. Opt. Phys.*, **1997**, 36, 289
7. Gryzinski, M.; *Classical theory of atomic collision, Part I, Theory of inelastic collisions*, *Phys. Rev. A*, **1967**, 138, 336
8. Roy, B. N.; Rai, D. K.; *Application of classical collision theory to electron impact double ionization of atoms*, *J. Phys. B : At. Mol. Phys.*, **1973**, 6, 816
9. Vriens, L.; *Case studies in atomic collision Physics, Binary Encounter and Classical collision theory*, (North Holland, Amsterdam), vol. 1, page 358, *Proc. Phys. Soc.*, **1969**, vol. 89, page 113
10. Chatterjee, S. N.; Roy, B. N.; *Electron impact double ionization of Ca and Sr*, *J. Phys. B : At. Mol. Opt. Phys.*, **1984**, 17, 2527
11. Chatterjee, S. N.; Roy, B. N.; *Electron impact double ionization of Ar^+ , Ar^{2+} and Xe^+* , *J. Phys. B : At. Mol. Opt. Phys.*, **1987**,20, 229
12. Jha, L. K.; Roy, B. N.; *Electron impact single and double ionization of Mg*, *EPJD*, **2002**, vol. 20, page 5
13. Jha, L. K.; Roy, B. N.; *Double ionization of singly and doubly charged Titanium ions by electron impact*, *Physica Scripta*, **2005**, 71,185
14. Minakshi, Jha, L. K.; Chatterjee, S. N.; *H^+ and He^{2+} impact single and double ionization of Pb*, *EPJD*, **2009**, 51,331
15. Singh, M. P.; Jha, L. K.; *Single and double ionization of Mg by H^+ and He^{2+} impact*, *Phys. Scr.*, **2009**, 80, 025302

16. Shah, M. B.; Patton, C. J.; Bolorizadeh, M. A.; Geddes, J.; Gilbody, H. B.; *J. Phys. B : At. Mol. Opt. Phys.* ,**1995**, 28, 1821
17. Kumar, A.; Roy, B. N.; *Application of the Binary Encounter theory to proton impact double ionization of atoms, J. Phys. B : At. Mol. Phys.* ,**1977**, 10, 3047
18. Kumar, A.; Roy, B. N.; *Proton impact double ionization of Noble gas atoms, J. Phys. B : At. Mol. Phys.* ,**1981**, 14, 501
19. Vriens, L.; *Binary Encounter proton atom collision theory, Proc. Phys. Soc.* ,**1967**, 90,935
20. Catlow G.; McDowel, M. R. C.; *Proc. Phys. Soc.* ,**1967**, 92, 875
21. Clementi, E.; Roetti, C.; *At. Data and Nucl. Data Tables*, **1974**, 14,177
22. Desclaux, J. P.; *At. Data and Nucl. Data Tables*,**1973**, 12,311
23. Patton, C. J.; Shah, M. B.; Bolorizadeh, M. A.; Geddes, J.; Gilbody, H. B.; *Ionization in collision of fast H^+ and He^{2+} ion impact with Fe and Cu atoms, J. Phys. B : At. Mol. Opt. Phys.* ,**1995**, 28, 3889